

# Scattering and Coupling Reduction of Dipole Antenna Using Gradient Index Metamaterial Based Cloak

Mahesh S. Bisht\* and Kumar V. Srivastava

**Abstract**—A gradient index metamaterial (GIM) based conformal cloak is utilized to reduce the overall scattering of a dipole antenna and its blockage effect when being placed in close proximity of a horn antenna. The reduction in scattering is attributed to wave conversion properties of GIM cover, by virtue of which the propagating waves get converted to surface waves and vice versa, thus reducing the scattering signature of the dipole. The GIM cover also has the advantage of larger bandwidth than single metasurface based cloaks (mantle cloak). The proposed GIM based cloak proves to be effective in reducing the mutual interference between dipole and horn antenna without disrupting the performance of individual antennas in their respective frequency band of interest. The Ansys HFSS simulation results are presented to demonstrate the effectiveness of GIM based cover to reduce mutual blockage effect between a low band dipole and an S-band horn antenna.

## 1. INTRODUCTION

There is a need of antennas with low scattering signature in applications related to sensing and monitoring systems. The use of antennas with low observability to electromagnetic waves greatly enhances the performance of such systems. Also it is highly desirable to have some mechanism to reduce the effect of an antenna on the performance of another antenna when they are placed in close proximity. For instance, when two antennas are placed in close proximity, there would be interference between the two. In the manuscript, we try to reduce the interference between the two antennas. In view of these applications, various approaches have been demonstrated to cloak the antenna and reduce its overall scattering width. In [1], the suppression of mutual blockage is demonstrated using a transmission line (TL) cloak wherein it is demonstrated that TL cloak is capable of hiding a mesh-like metal object placed inside it from the incident wave. However, the mantle cloaks, which are based on scattering cancellation approach, are more advantageous for rendering any object invisible to EM waves [2–5]. Hence, various works have been published related to reduction of scattering signature of antennas and sensors [6–9] based on mantle cloaks. For instance, in [7], mantle cloak was used to reduce the mutual interference between two dipole antennas. It is further extended to design a dual polarized mantle cloak for dipole antennas [9] wherein it is shown that the mutual blockage between closely placed log-periodic antenna and covered dipole antenna is reduced using mantle cloak. Mantle cloak has also been used to achieve transparency in printed circuit technology wherein mutual coupling between two monopoles was reduced using elliptically shaped mantle cloaks [10–14]. In addition to these works, in [15], cloaking of Yagi-Uda antenna has been demonstrated using scattering cancellation technique.

However, in the present work, the cloaking based on gradient index media (GIM) [16] is utilized for applications pertaining to reduction of mutual blockage between antennas placed in close proximity of each other. In an earlier work, we demonstrated the use of gradient index metamaterial for cloaking wherein the scattering due to a PEC cylinder was suppressed by enclosing it with conformal GIM

---

*Received 30 December 2019, Accepted 8 February 2020, Scheduled 20 March 2020*

\* Corresponding author: Mahesh S. Bisht (msbisht@iitk.ac.in).

The authors are with the Department of Electrical Engineering, Indian Institute of Technology Kanpur, Uttar Pradesh 208016, India.

based shell with spatially varying permittivity ( $\epsilon$ ) and permeability ( $\mu$ ) profiles [16]. The cloaking behaviour was attributed to the mechanism of conversion of propagating waves into surface waves and vice-versa [16–19]. To achieve this, the GIM based cover was designed by arranging supercells with spatially varying  $\epsilon$  and/or  $\mu$  profiles around the object in such a way that as the EM wave reaches the cover, it gets converted to surface waves and again back to propagating waves while leaving the cloak. The GIM based cloak is also advantageous because of its large bandwidth as compared to single metasurface based cloaks (mantle cloaks) [16]. It was also shown in [16] that the frequency of operation and bandwidth can be controlled by tailoring the permittivity and permeability profiles and also by varying the thickness of GIM cloak.

Hence, in this paper, GIM based cloaking is utilized for reduction of mutual coupling, when a dipole is placed in close proximity of another antenna operating in a frequency band different from that of the dipole antenna. For instance, the GIM cloak is designed such that it reduces the effect of dipole antenna on performance of an S-band horn antenna. Section-2 presents a design procedure of dipole antenna and its GIM cover together with the effects of GIM cover on its performance. This section further includes the scattering analysis of bare dipole antenna and when it is covered by GIM shell, under plane wave excitation. In Section-3, the effectiveness of GIM cloaking is demonstrated by considering the case when GIM covered dipole antenna is placed in close proximity of an S-band horn antenna. Several simulation results (done in Ansys HFSS) are presented to show that the mutual coupling between dipole antenna and horn is greatly reduced within the operation band of horn antenna while keeping the performance of bare dipole antenna unaltered.

## 2. DESIGN OF GIM SHELL FOR DIPOLE ANTENNA

This section deals with the design of a GIM based cloaking shell for a dipole antenna. It is shown that when dipole antenna is covered with a GIM material around it, its resonant frequency changes and shifts towards the lower side. The amount of shift depends upon the thickness of GIM shell (though not shown for brevity). As the thickness of GIM shell increases, the resonant frequency shifts more towards lower frequency side. Thus, it is necessary to design a bare dipole at a little higher frequency such that it comes down to desired operating frequency range when being covered with GIM cloak. The geometry of bare dipole and gradient index metamaterial (GIM) covered dipole antenna is shown in Fig. 1(a) and Fig. 1(b), respectively. The GIM shell consists of four supercells [16] arranged around the periphery of dipole as depicted in Fig. 1(c). The arrangement of supercells is such that it converts the impinging propagating wave to surface wave and vice versa on exit through the dipole, thus reducing the scattering signature of the dipole.

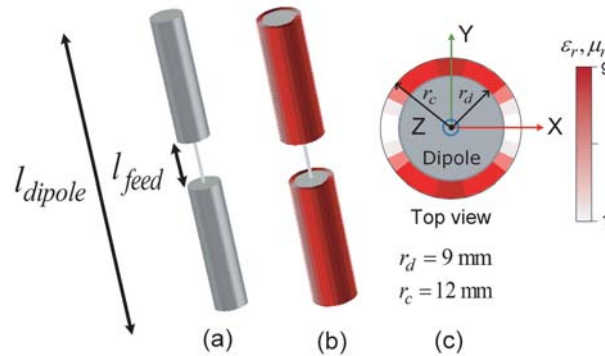


**Figure 1.** (a) Bare dipole antenna of radius,  $r_d = 9$  mm, (b) when it is covered with gradient index metamaterial cover of thickness,  $h = r_c - r_d = 3$  mm, and (c) the schematic wherein color gradient represents the variation of permittivity and/or permeability around the GIM cover.

In this paper, a GIM cover is designed to reduce the scattering signature of a dipole antenna in S-band. It means that the thickness and corresponding permittivity/permeability profiles of GIM shell are chosen such that it effectively operates within the S-band. Thus, the thickness of GIM cloak is

chosen to be equal to  $h = r_c - r_a = 3$  mm, and the permittivity and permeability profiles are chosen as  $\mu_r = \epsilon_r = 1 + \kappa x/2k_0h$  where  $\kappa = 2.8k_0$  is the phase constant along the metamaterial, and  $k_0$  is the phase constant of the incident wave in free space. The procedure to get the GIM cover is as follows: The permittivity and permeability profiles are calculated in the Cartesian domain only for a single supercell, using  $\mu_r = \epsilon_r = 1 + \kappa x/2k_0h$  from  $x = 0$  to  $x = L$ , indicated as ‘Supercell-1’ in Fig. 2. It means that the above expression is valid only within a supercell of length,  $L = 18.85$  mm [16]. The ‘Supercell-1’ is then mirror imaged at  $x = L$  plane to obtain the second supercell. Both of these supercells together are then mirror imaged at  $x = 2L$  plane to obtain the entire GIM cover. Hence, the GIM cover consists of four supercells. Within a supercell, the continuous  $\epsilon_r$  and  $\mu_r$  variation is discretized into seven unit-cells with constant permittivity/permeability, as depicted by the staircase profile in Fig. 2. Subsequently, the GIM is wrapped around the cylinder (dipole antenna in the present case) to obtain the cloaking cover.  $\epsilon_r$  and  $\mu_r$  values range from 1 to 8.5 in a supercell. The dipole antenna is designed to operate in the frequency range of 0.65 – 0.85 GHz in the presence of a GIM cover. Thus, the proposed GIM covered dipole works just fine as bare dipole in low frequency band and at the same time possesses reduced scattering signature in S-band.

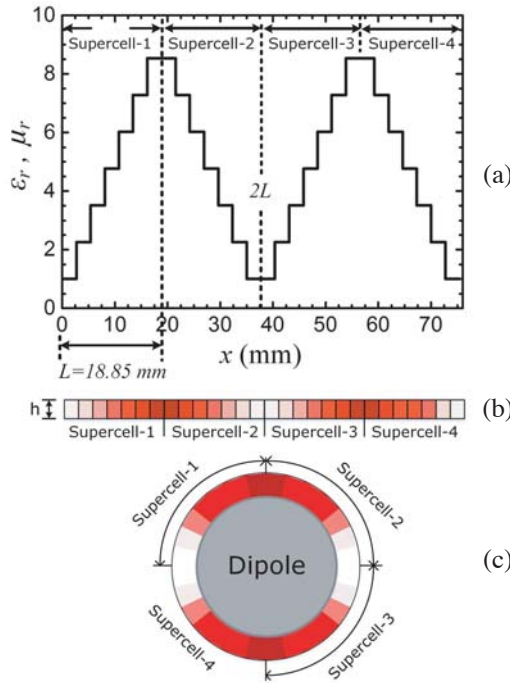


**Figure 2.** (a) The discretized permittivity and permeability profile for the GIM cover used to reduce the scattering of dipole antenna. Here  $L$  is the length of a supercell, and the whole of GIM cover consists of four supercells as shown in (b), wherein supercells are alternatively arranged as their mirror images, and (c) the planar GIM is wrapped around the dipole to obtain the required GIM cover.

Next,  $S_{11}$  plots for the bare and GIM covered dipole antennas are shown in Fig. 3. An observation can be made that the resonance point for GIM covered dipole antenna is shifted towards the lower frequency as compared to bare dipole antenna because the presence of GIM cover changes the input impedance of dipole and lowers the frequency at which the reactance part of input impedance becomes zero, hence the shift in resonance. Owing to this effect, it is imperative to choose the dimensions of bare dipole antenna such that it operates at a little higher than the desired frequency. In this way, when it is covered with GIM shell, it will operate in the desired frequency band. Keeping this in mind, the dimensions of bare dipole are taken as:  $l_{dipole} = 138.8$  mm,  $l_{feed} = 10$  mm, for which resonance occurs at 0.93 GHz while for GIM covered dipole it occurs at a frequency of 0.75 GHz.

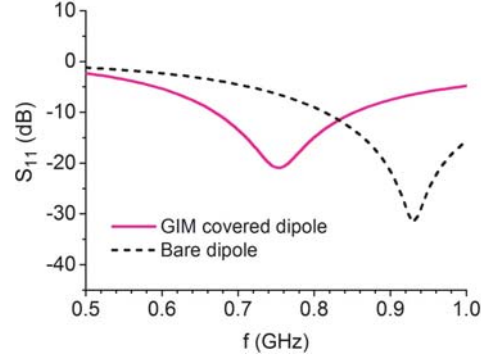


**Figure 3.**  $S_{11}$  plots of bare and GIM covered dipole antennas.

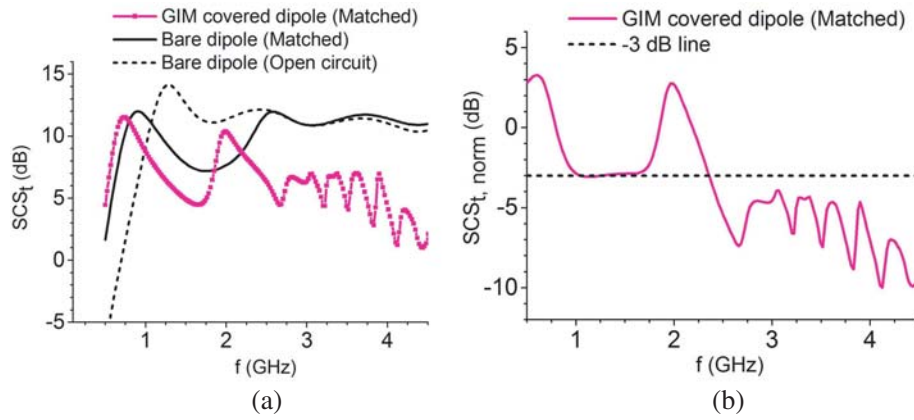


**Figure 4.** (a) Total scattering cross-section ( $SCS_t$ ) plots depicting reduction in scattering, for GIM covered dipole, within the S-band, and (b) normalized total scattering cross-section ( $SCS_{t,norm}$ ) plots where normalization is done with respect to matched terminated bare dipole antenna.

### 2.1. Scattering Analysis of Bare and GIM Covered Dipole

Here the scattering behaviour of bare and GIM covered dipole antennas is presented under the influence of plane waves. The plots for total scattering width versus frequency are plotted in Fig. 4(a) and Fig. 4(b). The total scattering width is obtained by integrating scattering cross-section around the dipole geometry through all angles along azimuthal direction. These plots are obtained for the case when a plane wave is incident on the dipole with its  $E$ -field vector oriented along the dipole axis (i.e.,  $Z$ -axis). The simulations are done in commercially available software Ansys HFSS. The plot in Fig. 4(a) consists of three curves which are for: (a) GIM covered dipole antenna with matched load, (b) bare dipole antenna terminated with matched load at its terminal, (b) open circuited bare dipole antenna, respectively. The plots in Fig. 4(b) are normalized plots for the matched terminated scenario, wherein normalization is done with respect to matched terminated bare dipole antenna.

It can be observed from Fig. 4(a) that the total scattering width for the GIM covered dipole antenna decreases at frequencies corresponding to S-band while keeping the resonance at lower frequency band unaltered [9]. The reduced scattering signature can be more clearly depicted from Fig. 4(b) wherein the scattering width plots for GIM covered dipole are normalized with respect to that for bare dipole antenna. There is a reduction in scattering signature with a good 3 dB bandwidth that appropriately covers the S-band. Hence, it is envisaged that the proposed GIM cover can be effectively used to reduce the scattering signature of dipole antenna when it is placed in close proximity of any S-band antenna. To better illustrate the scattering reduction, the plots of scattering cross-section around the bare and GIM covered dipoles are presented in Fig. 5 for two frequencies within S-band, i.e.,  $f = 2.9$  GHz (Fig. 5(a)

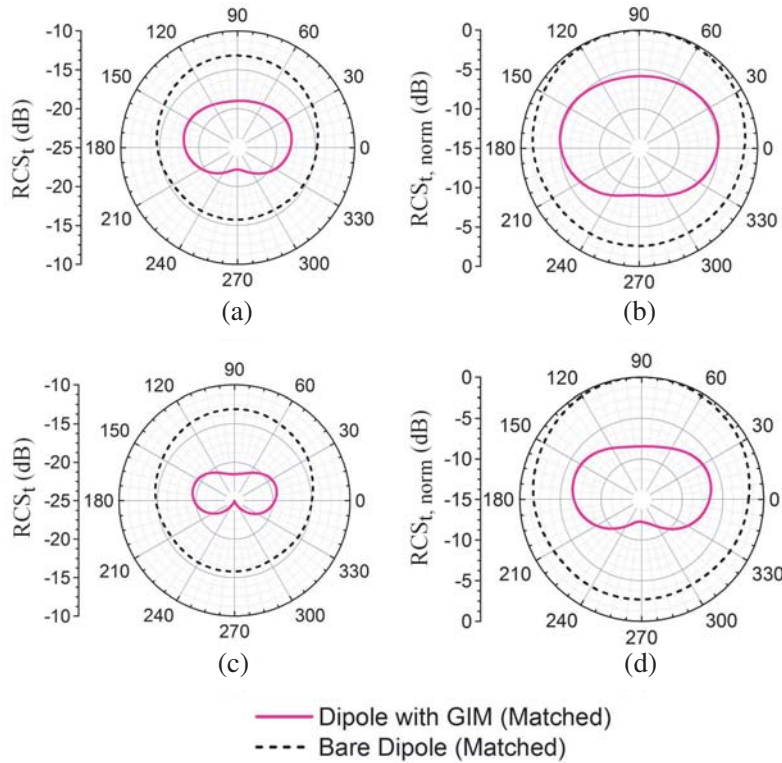


**Figure 5.** Scattering patterns around the GIM covered and bare dipole antennas under matched termination conditions, for two frequencies within S-band: (a), (b) 2.9 GHz and (c), (d) 3.2 GHz. The plots in (b) & (d) are normalized versions of plots in (a) & (c), respectively. The normalization is done with respect to maximum scattering due to bare dipole antenna.

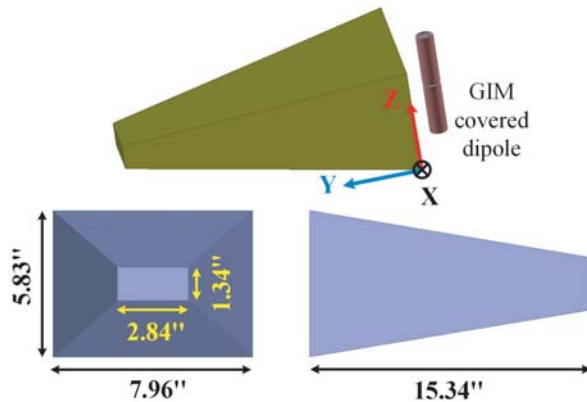


**Figure 6.** (Top) Simulation setup when GIM covered and bare dipoles are placed in front of an S-band horn antenna; (Bottom) Geometrical dimensions of the horn.

and Fig. 5(b)) and  $f = 3.2$  GHz (Fig. 5(c) and Fig. 5(d)). The plots in Fig. 5(b) and Fig. 5(d) are normalized with respect to the maximum scattering due to bare dipole antenna. It can be observed that in the presence of GIM cover, the scattering cross-section decreases quite effectively in all directions.

### 3. SIMULATIONS IN S-BAND

In this section, the simulations are presented for the cases when a bare dipole antenna and a GIM covered dipole are placed in close proximity of an S-band horn antenna. All the simulations are performed in

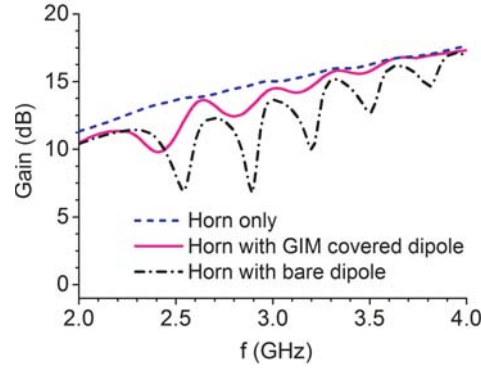


**Figure 7.** Gain versus frequency plots when GIM covered and bare dipole antennas are placed in close proximity of S-band horn antenna.

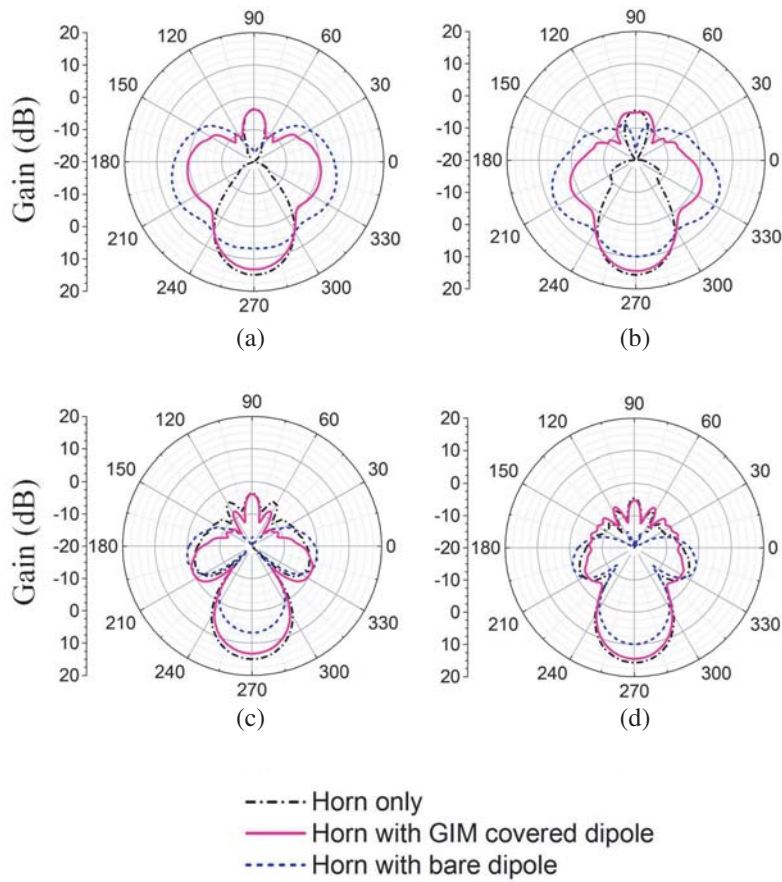


**Figure 8.** Gain patterns of horn antenna in presence of GIM covered and bare dipoles: (Top)  $\theta = 90^\circ$  plane, and (Bottom)  $\phi = 90^\circ$  plane, for  $f = 2.9$  GHz [(a), (c)], and  $f = 3.2$  GHz [(b), (d)], respectively.

Ansyz HFSS. Firstly, the horn antenna is designed, and its dimensions are optimized for adequate performance within the S-band (geometry of horn antenna is shown in Fig. 6 with required dimensional parameters). It is then followed by simulations with bare and GIM covered dipole antennas placed in close proximity of horn antenna. The simulation setup used is as shown in Fig. 6 wherein a GIM covered dipole antenna is placed in front of the horn with a gap of 25 mm between the outer surface of GIM cover and horn antenna top face. The simulation domain is terminated using radiation boundary conditions.

The dimensions of horn antenna are taken from L3 Narda-ATM Microwaves specification sheet for WR284 waveguide size and a gain of 15 dB. According to specifications given in website [20], the horn antenna operates within the frequency band of 2.6–3.95 GHz. The results of these simulations are depicted in Fig. 7 and Fig. 8, respectively.

The gain versus frequency is plotted in Fig. 7, where it can be observed that the gain of horn antenna is restored nicely when the dipole is covered with the gradient index metamaterial as opposed to when a bare dipole is placed in front of it. To further strengthen our viewpoint, the gain patterns for horn antenna in the presence of GIM covered and bare dipoles are presented in Fig. 8. It can be seen that the distortion in gain patterns is restored nicely when bare dipole antenna is covered with the proposed GIM cloak. The plots in Fig. 7 and Fig. 8 correspond to the case when bare dipole and GIM covered dipole both are matched and terminated at their terminals.

These encouraging results make the GIM cloaking a potential candidate for reducing mutual interference between closely placed antennas, for instance, in a crowded communication system. Also, in the present case, the main advantage is that permittivity and permeability values are isotropic, positive, and do not have very high values (the values for both  $\epsilon_r$  and  $\mu_r$  range from 1 to 8.5). So, there is no need to design unit-cell based metamaterials. Instead, there are chemical techniques that can be used to manipulate the permittivity and permeability values of a host medium. For instance, by mixing Barium Titanate with Polydimethylsiloxane (PDMS), a flexible dielectric composite material can be prepared. It has an additional advantage that the permittivity can be controlled by varying the concentration of Barium Titanate in the composite [21–24]. Also, using similar chemical approaches, a composite can be prepared wherein permittivity and permeability of the material can be varied simultaneously, as demonstrated by various research groups [25–28]. Hence, with the use of these magneto-dielectric composites, it is possible to realize the GIM cloak for the current purpose.

#### 4. CONCLUSIONS

A gradient index metamaterial (GIM) based conformal cloak is utilized to reduce the overall scattering of dipole antenna within S-band and also its blockage effect when being placed in close proximity of an S-band horn antenna. The proposed GIM based cloak proves to be effective in reducing the mutual interference without disrupting the performance of individual antennas (dipole and horn) in their respective frequency band of interest. Also, the values of permittivity and permeability, in the present case, are isotropic and positive. So, there is no need to go for unit-cell based metamaterials for its realization. Instead, available chemical techniques can be used to realize flexible magneto-dielectric substrates. These promising results render the proposed GIM cover suitable for scattering or blockage reduction of dipole antenna in crowded communication systems.

#### REFERENCES

1. Vehmas, J., P. Alitalo, and S. A. Tretyakov, "Experimental demonstration of antenna blockage reduction with a transmission-line cloak," *IET Microwaves, Antennas Propagation*, Vol. 6, No. 7, 830–834, 2012.
2. Alù, A. and N. Engheta, "Achieving transparency with plasmonic and metamaterial coatings," *Phys. Rev. E*, Vol. 72, No. 1, 2005.
3. Alù, A., "Mantle cloak: Invisibility induced by a surface," *Phys. Rev. B*, Vol. 80, No. 24, 2009.
4. Chen, P. Y. and A. Alù, "Mantle cloaking using thin patterned metasurfaces," *Phys. Rev. B*, Vol. 80, No. 24, 2011.
5. Padooru, Y. R., A. B. Yakovlev, P. Y. Chen, and A. Alù, "Analytical modeling of conformal mantle cloaks for cylindrical objects using sub-wavelength printed and slotted arrays," *Journal of Applied Physics. B*, Vol. 112, No. 3, 2012.
6. Alù, A. and N. Engheta, "Cloaking a sensor," *Phys. Rev. Lett.*, Vol. 102, No. 23, 2009.
7. Monti, A., J. Soric, A. Alù, F. Bilotti, A. Toscano, and L. Vegni, "Overcoming mutual blockage between neighboring dipole antennas using a low-profile patterned metasurface," *IEEE Antennas and Wireless Propagation Letters*, Vol. 11, 1414–1417, 2012.

8. Soric, J. C., R. Fleury, A. Monti, A. Toscano, F. Bilotti, and A. Alù, "Controlling scattering and absorption with metamaterial covers," *IEEE Transactions on Antennas and Propagation*, Vol. 62, No. 8, 4220–4229, 2014.
9. Soric, J. C., A. Monti, A. Toscano, F. Bilotti, and A. Alù, "Dual-polarized reduction of dipole antenna blockage using mantle cloaks," *IEEE Transactions on Antennas and Propagation*, Vol. 63, No. 11, 4827–4834, 2015.
10. Bernety, H. M. and A. B. Yakovlev, "Cloaking of single and multiple elliptical cylinders and strips with confocal elliptical nanostructured graphene metasurface," *Journal of Physics: Condensed Matter*, Vol. 27, No. 18, 2015.
11. Bernety, H. M. and A. B. Yakovlev, "Decoupling antennas in printed technology using elliptical metasurface cloaks," *Journal of Applied Physics*, Vol. 119, No. 1, 2016.
12. Monti, A., J. C. Soric, B. Mirko, R. Davide, V. Stefano, F. Trotta, A. Alù, A. Toscano, and F. Bilotti, "Mantle cloaking for co-site radio-frequency antennas," *Applied Physics Letters*, Vol. 108, No. 11, 2016.
13. Moreno, G., H. Bernety, and A. B. Yakovlev, "Wideband elliptical metasurface cloaks in antenna technology," *2017 IEEE International Symposium on Antennas and Propagation USNC/URSI National Radio Science Meeting*, 69–70, 2017.
14. Moreno, G., A. B. Yakovlev, H. M. Bernety, D. H. Werner, H. Xin, A. Monti, F. Bilotti, and A. Alù, "Wideband elliptical metasurface cloaks in printed antenna technology," *IEEE Transactions on Antennas and Propagation*, Vol. 66, No. 7, 3512–3525, 2018.
15. Monti, A., J. Soric, A. Alù, T. Alessandro, and B. Filiberto, "Design of cloaked Yagi-Uda antennas," *EPJ Applied Metamaterials*, Vol. 3, 2016.
16. Bisht, M. S. and K. V. Srivastava, "Design and analysis of gradient index metamaterial-based cloak with wide bandwidth and physically realizable material parameters," *Applied Physics A*, Vol. 124, No. 4, 2018.
17. Shulin, S., H. Qiong, X. Shiyi, X. Qin, L. Xin, and Z. Lei, "Gradient-index meta-surfaces as a bridge linking propagating waves and surface waves," *Nature Materials*, Vol. 11, 2012.
18. Xu, Y., C. Gu, B. Hou, Y. Lai, J. Li, and H. Chen, "Broadband asymmetric waveguiding of light without polarization limitations," *Nature Communications*, Vol. 4, 2013.
19. Gu, C., Y. Xu, S. Li, W. Lu, J. Li, H. Chen, and B. Hou, "A broadband polarization-insensitive cloak based on mode conversion," *Scientific Reports*, Vol. 5, 2015.
20. L3 Narda-ATM, "Waveguide horn antenna-standard gain and wide band," <https://www.atmmicrowave.com/waveguide/horn-antenna-standard-gain-wide-band>.
21. Saini, L., Y. Janu, M. K. Patra, R. K. Jani, G. K. Gupta, A. Dixit, and S. R. Vadera, "Dual band resonance in tetragonal BaTiO<sub>3</sub>/NBR composites for microwave absorption applications," *J. Am. Ceram. Soc.*, Vol. 99, No. 9, 3002–3007, 2016.
22. Bele, A., M. Cazacu, G. Stiubianu, and S. Vlad, "Silicone-barium titanate composites with increased electromechanical sensitivity. The effects of the filler morphology," *RSC Adv.*, Vol. 4, No. 102, 58522–58529, 2014.
23. Murugan, M., V. K. Kokate, M. S. Bapat, and A. M. Sapkal, "Synthesis of nanosized barium titanate/epoxy resin composites and measurement of microwave absorption," *Bull. Mater. Sci.*, Vol. 33, No. 6, 657–662, Dec. 2010.
24. Babar, A. A., V. A. Bhagavati, L. Ukkonen, A. Z. Elsherbeni, P. Kallio, and L. Sydanheimo, "Performance of high-permittivity ceramic-polymer composite as a substrate for UHF RFID tag antennas," *Int. J. Antennas Propag.*, 2012.
25. Vural, M., B. Crowgey, L. C. Kempel, and P. Kofinas, "Nanostructured flexible magneto-dielectrics for radio frequency applications," *J. Mater. Chem. C*, Vol. 2, No. 4, 756–763, 2014.
26. Han, K., M. Swaminathan, R. Pulugurtha, H. Sharma, R. Tummala, S. Yang, and V. Nair, "Magneto-dielectric nanocomposite for antenna miniaturization and SAR reduction," *IEEE Antennas and Wireless Propagation Letters*, Vol. 15, 72–75, 2016.

27. Morales, C. A., "Magneto-dielectric polymer nanocomposite engineered substrate for RF and microwave antennas," Ph.D. Dissertation, University of South Florida, 2011.
28. Yang, T. I., R. N. C. Brown, L. C. Kempel, and P. Kofinas, "Controlled synthesis of core-shell iron-silica nanoparticles and their magneto-dielectric properties in polymer composites," *Nanotechnology*, Vol. 22, No. 10, 2011.